Biofuels and Environmental Biotechnology **Biotechnology and Bioengineering**
DOI 10.1002/bit.26558

Improving methyl ketone production in *E. coli* by heterologous expression of NADH-dependent FabG†

Ee-Been Goh[1,2], Yan Chen[1,2], Christopher J. Petzold[1,2], Jay D. Keasling[1,2,3,4], and Harry R. Beller*[1,5]

[1]Joint BioEnergy Institute (JBEI), 5885 Hollis Street, Emeryville, CA 94608
[2]Biological Systems & Engineering Division, Lawrence Berkeley National Laboratory, Berkeley, CA 94720
[3]Departments of Chemical & Biomolecular Engineering and of Bioengineering, University of California, Berkeley, CA 94720
[4]The Novo Nordisk Foundation Center for Biosustainability, Technical University of Denmark, Kogle Allee, DK2970-Hørsholm, Denmark
[5]Earth and Environmental Sciences, Lawrence Berkeley National Laboratory, Berkeley, CA 94720

***Corresponding author:**

Harry R. Beller
Joint BioEnergy Institute
5885 Hollis Street
Emeryville, CA 94608

E-mail HRBeller@lbl.gov
Phone (510) 486-7321
Fax (510) 486-5686

†This article has been accepted for publication and undergone full peer review but has not been through the copyediting, typesetting, pagination and proofreading process, which may lead to differences between this version and the Version of Record. Please cite this article as doi: [10.1002/bit.26558]

Additional Supporting Information may be found in the online version of this article.

Received November 21, 2017; Revision Received January 22, 2018; Accepted January 31, 2018

Abstract

We previously engineered *E. coli* to overproduce medium- to long-chain saturated and monounsaturated methyl ketones, which could potentially be applied as diesel fuel blending agents or in the flavor and fragrance industry. Recent efforts at strain optimization have focused on cofactor balance, as fatty acid-derived pathways face the systematic metabolic challenge of net NADPH consumption [in large part, resulting from the key fatty acid biosynthetic enzyme FabG (β-ketoacyl-ACP reductase)] and net NADH production. In this study, we attempted to mitigate cofactor imbalance by heterologously expressing NADH-dependent, rather than NADPH-dependent, versions of FabG identified in previous studies. Of the four NADH-dependent versions of FabG tested in our previously best-reported methyl ketone-producing strain (EGS1895), the version from *Acholeplasma laidlawii* (Al_FabG) showed the greatest increase in methyl ketone yield in shake flasks (35-75% higher than for an RFP negative-control strain, depending on sugar loading). An improved strain (EGS2920) attained methyl ketone titers during fed-batch fermentation of 5.4 ± 0.5 g/L, which were, on average, ca. 40% greater than those for the base strain (EGS1895) under fermentation conditions optimized in this study. Shotgun proteomic data for strains EGS2920 and EGS1895 during fed-batch fermentation were consistent with the goal of alleviating NADPH limitation through expression of Al_FabG. For example, relative to strain EGS1895, strain EGS2920 significantly upregulated glucose-6-phosphate isomerase (directing flux into glycolysis rather than the NADPH-producing pentose phosphate pathway) and downregulated MaeB (a $NADP^+$-dependent malate dehydrogenase). Overall, the results suggest that heterologous expression of NADH-dependent FabG in *E. coli* may improve sustained production of fatty acid-derived renewable fuels and chemicals.

Keywords

Cofactor balance, methyl ketones, NADPH, NADH-dependent FabG, shotgun proteomics

This article is protected by copyright. All rights reserved

1. Introduction

Research on microbial production of biofuels and renewable chemicals over the past decade has included the development of fatty acid-derived molecules, such as fatty acid alkyl esters, medium- and short-chain methyl ketones, alkanes, α-olefins, long-chain internal alkenes, and fatty alcohols (Beller et al., 2015; Handke et al., 2011; Janßen and Steinbüchel, 2014; Lennen and Pfleger, 2013). Although relatively good performance has been attained for some of these compounds (e.g., 40% of maximum theoretical yield; Goh et al. 2014), the fatty acid biosynthetic pathway presents metabolic challenges, particularly in maintaining intracellular redox balance among nicotinamide adenine dinucleotide (NAD) cofactors. The primary demand for NADPH in *E. coli*'s fatty acid biosynthetic pathway derives from two reductases, FabG (β-ketoacyl-ACP reductase) and potentially, FabI (enoyl-ACP reductase). Whereas FabI displays activity with both NADH and NADPH (Bergler et al., 1996), FabG, which belongs to the short-chain dehydrogenase/reductase enzyme family, is active only with NADPH in characterized versions (Toomey and Wakil, 1966). Using biosynthesis of a C_{13} methyl ketone (2-tridecanone) as an example of fatty acid-related cofactor requirements, production from glucose (*via* tetradecanoic acid) in *E. coli* using a previously developed pathway (Goh et al., 2014) would consume substantial NADPH while generating excess NADH. Specifically, biosynthesis of 1 mol of 2-tridecanone from glucose would result in net consumption of 6 (or 12) mol of NADPH and net production of 9 (or 15) mol of NADH, depending on FabI cofactor usage. Such cofactor imbalance may not only cause cessation of important biochemical reactions within the cell but also result in oxidative stress (Auriol et al., 2011; Chou et al., 2015; Spaans et al., 2015).

Some of our earlier metabolic engineering efforts to improve production of diesel-range methyl ketones in *E. coli* were primarily focused on driving carbon flux towards fatty acid and

methyl ketone synthesis, which included genetic modifications such as: (a) overproduction of β-ketoacyl-coenzyme A (CoA) thioesters achieved by modification of the β-oxidation pathway (specifically, overexpression of a heterologous acyl-CoA oxidase and native FadB, and chromosomal deletion of *fadA*), (b) overexpression of a native thioesterase (FadM), and (c) increasing fatty acid flux into the β-oxidation pathway by overexpression of FadR and FadD (Goh et al., 2014, 2012) (Figure S1). Further efforts, including consolidation of overexpressed genes into one plasmid, codon optimization, and chromosomal deletion of key acetate production pathways, resulted in an *E. coli* strain (EGS1895) that attained 40% of the maximum theoretical yield. More recently, we have shifted our focus towards cofactor imbalance, specifically consumption of NADPH during fatty acid biosynthesis. Researchers have used a variety of strategies to address redox imbalance and cofactor usage, including altering the global availability of cofactors through metabolic engineering of the pentose phosphate pathway or overexpression of NADH oxidases, kinases, or transhydrogenases (Lee et al., 2009, 2013; Wang et al., 2013; Zerez et al., 1987).

In this study, we describe a different strategy for alleviating high NADPH consumption and related cofactor imbalance: circumventing the NADPH requirement from the native *E. coli* FabG by overexpressing recently discovered NADH-dependent versions of FabG (Javidpour et al., 2014). More specifically, we expressed four NADH-dependent versions of FabG in our previously best-reported methyl ketone-producing strain (EGS1895), and after identification of the most productive FabG version (from *Acholeplasma laidlawii*), conducted strain optimization of two- versus one-plasmid systems and variable positioning of *fabG* within the single plasmid. Finally, we conducted extensive shotgun proteomic studies of our best-performing strain (EGS2920; 5.4 ± 0.5 g/L during fed-batch fermentation) versus strain EGS1895 in fed-batch

mode to better understand the physiological differences that led to improved methyl ketone production in strain EGS2920 relative to strain EGS1895. This study differs from a previous investigation of NADH-dependent FabG (Javidpour et al., 2014) in several important aspects: (1) the previous study focused on a NADH-dependent FabG version from *Cupriavidis taiwanensis*, not *A. laidlawii*, based solely on its *in vitro* performance, (2) the previous study employed anaerobic conditions for production studies, (3) the previous study used a less optimized methyl ketone-producing base strain that had 160-fold lower titer than the strain used in the present study (EGS1895), (4) optimized versions of strains expressing *A. laidlawii fabG* were constructed and tested in the present study, and (5) production tests in the present study involved fed-batch fermentation and shotgun proteomic characterization.

2. Materials and Methods

2.1 Bacterial strains, plasmids, oligonucleotides, and reagents

Bacterial strains and plasmids used in this study are listed in Table I. Strains and plasmids along with their associated information (annotated GenBank-format sequence files) have been deposited in the public version of the JBEI Registry (https://public-registry.jbei.org; entries JPUB_XXXX [to be added in proofs]) and are physically available from the authors and/or Addgene (http://www.addgene.org) upon request. Primer sequences and coding sequences for amplification of the *rex* repressor gene from *S. aureus* RN4220 and the alternate *fabG* versions are listed in Tables S1 and S2 (Appendix A).

2.2 Plasmid and strain construction for expression in E. coli

Amplification of the *S. aureus rex* gene and the variant *fabG* genes was carried out by colony PCR of the applicable strains (Table I), with appropriate primers (Table S1), as previously described (Goh et al., 2012), and the amplicons were assembled into expression

plasmids by Gibson assembly (Gibson et al., 2009). Proper clone construction was confirmed by colony PCR followed by Sanger sequencing of the purified plasmid DNA, which was performed by GENEWIZ, Inc. (Berkeley, CA).

2.3 Media and bacterial growth

Cultivation of *E. coli* was performed aseptically as previously described (Sambrook et al., 1989). *E. coli* DH10B cells were used for cloning and lysogeny broth (LB) was used for routine growth and propagation of strains. When required, antibiotics were added to the growth medium at the following final concentrations: chloramphenicol, 25 μg/mL; kanamycin, 50 μg/mL. For shake-flask production experiments, M9-MOPS minimal medium [M9 medium supplemented with 75 mM MOPS, 2 mM $MgSO_4$, 1 mg/L thiamine, 10 nM $FeSO_4 \cdot 7H_2O$, 0.1 mM $CaCl_2 \cdot 2H_2O$, 74.1 mM NH_4Cl and micronutrients consisting of 30 nM $(NH_4)_6Mo_7O_{24}$, 4 μM boric acid, 30 nM $CoCl_2$, 15 nM $CuSO_4$, 80 nM $MnCl_2$, and 10 nM $ZnSO_4$] with 10 g/L or 20 g/L glucose as the sole carbon source was used for production (Zhang et al., 2012). Prior to production in M9-MOPS minimal medium, strains were first adapted as previously described (Goh et al., 2014).

2.4 Methyl ketone production experiments in shake flasks

Prior to production in shake flasks, an aliquot of the previously frozen M9-MOPS-adapted glycerol stock was used to inoculate 5 mL of M9-MOPS 1% glucose medium in a test tube to cultivate an overnight starter culture. At the start of production, the overnight culture was diluted to a final OD_{600} of ~0.01 into 50 mL of M9-MOPS medium with either 1% or 2% glucose in a 250-mL flat-bottom flask. Cultures were incubated at 37ºC on a shaking platform with 200-rpm agitation. The cultures were induced at 6 hr with 0.5 mM IPTG (isopropyl β-D-1-thiogalactopyranoside) and 1 mM arabinose. Immediately after induction, 2.5 mL of decane (Sigma-Aldrich, ReagentPlus, ≥ 99% purity) amended with 1 mg/mL of 3-tetradecanone (Sigma-

Aldrich) and 5 mg/L of perdeuterated tetracosane ($C_{24}D_{50}$, Sigma-Aldrich) as internal standards, was also added to the cultures.

At specific time points, 50 µL of the decane overlay was removed to quantify methyl ketones by gas chromatography-mass spectrometry (GC-MS). Culture samples were also removed for OD_{600} measurement, and for sugar and organic acid analysis by high performance liquid chromatography (HPLC). Details of GC-MS and HPLC analyses were described previously (Goh et al., 2014). Methyl ketones were quantified using the MassHunter quantitative analysis software and final concentrations of methyl ketones were normalized to the 3-tetradecanone internal standard that was initially amended in the decane or dodecane. Metabolites measured by HPLC were quantified by using external standard calibration with authentic standards.

2.5 Fed-batch fermentation in 2-L bioreactors for methyl ketone production

Fed-batch fermentation was carried out in a 2-L bioreactor equipped with a Sartorius BIOSTAT® B plus control unit for regulating dissolved oxygen (DO), pH, and temperature. A 50-mL M9-MOPS overnight culture prepared from a frozen glycerol stock of the M9-MOPS-adapted cells was cultured in a 250-mL flask, as previously described. This culture was used to inoculate 1.25 L of medium in the bioreactor. The medium for batch phase was adapted from Korz *et. al.* (Korz et al., 1995) and was composed of M9 salts (6.8 g/L Na_2HPO_4, 3.0 g/L KH_2PO_4, 1.0 g/L NH_4Cl, 0.5 g/L NaCl) supplemented with 0.5 g/L of $MgSO_4 \cdot 7H_2O$, 0.18 g/L of NH_4Cl, 1.0 mg/L thiamine, 10 nM of $FeSO_4 \cdot 7H_2O$, 100 µM $CaCl_2 \cdot 2H_2O$, micronutrients (as described above), 20 g/L of glucose, and appropriate antibiotics. The temperature of the bioreactor was maintained at 37ºC throughout the fermentation and the culture was maintained at pH 6.5 automatically by the addition of a 10 M potassium hydroxide solution. The initial stir rate

and airflow were set at 400 rpm and 0.72 VVM (volume of air per volume of liquid per minute), respectively. Dissolved oxygen was maintained above 40% of saturation *via* cascade control of air-flow rate (up to 2.0 VVM), followed by adjustment of stirrer speed (up to 1600 rpm). Cultures were induced with 1 mM arabinose and 0.5 mM IPTG at 6 hr after initiation of batch phase. In addition, 150 mL of dodecane (Sigma-Aldrich, ReagentPlus ≥ 99% purity) amended with 3 mg/mL of 3-tetradecanone (Sigma-Aldrich) as an internal standard, was added into the bioreactors. Batch phase was carried out until glucose was depleted (between 30 - 45 hr), at which time glucose feeding was initiated. The feed solution contained approximately 200 g/L glucose, 5 g/L $MgSO_4 \cdot 7H_2O$, 10.7 g/L NH_4Cl, trace elements [consisting of 16 mg/L EDTA, 3.8 mg/L $CoCl_2 \cdot 6H_2O$, 22.5 mg/L $MnCl_2 \cdot 4H_2O$, 2.3 mg/L $CuCl_2 \cdot 2H_2O$, 4.5 mg/L boric acid, 16.3 mg/L $Zn(CH_3COO)_2 \cdot 2H_2O$, 161 mg/L ferrous citrate], 3 mg/L thiamine, 1 mM arabinose, 0.5 mM IPTG, and appropriate antibiotics. Glucose feeding was carried out by a Watson-Marlow DU520 peristaltic pump set at a constant feed rate of 0.048 mL/min to 0.056 mL/min until all feed solution had been added (ca. 500 mL).

At specific time points, 10- to 15-mL samples were removed from the bioreactors *via* a syringe affixed to the sampling tube while the stirrer was still operating. Approximately 50 µL of cell cultures were filtered through a 0.2-µm pore-size syringe membrane filter directly into a vial for HPLC analysis and the rest of the cultures transferred to a 15-mL Falcon tube. After allowing the samples to sit in the 15-mL tube for 1 min, the supernatant dodecane overlay was pipetted out into a 2-mL microcentrifuge tube and centrifuged at 21,130 x *g* for 10 min to obtain a better-resolved aqueous-organic interface. The dodecane overlay was transferred into a glass vial and stored at 4ºC until GC-MS analysis.

2.6 Cell dry weight analysis of bioreactor samples

To determine the cell dry weight (CDW) of bioreactor samples, 5 mL of cell culture was filtered through a pre-weighed 0.45-µm Millipore cellulose acetate membrane and rinsed twice with 5 mL of reagent water (18 MΩ resistance; obtained from a Barnstead Nanopure system; Thermo Scientific, Waltham, MA). The filtered cells and membrane were baked in a 100ºC oven and re-weighed after 48 hr. The CDW was calculated by subtracting the weight of the empty membrane from the final weight of the dried cells and membrane.

2.7 Quantification of intracellular concentration of redox cofactors during fermentation

The intracellular concentrations of NAD^+, NADH, $NADP^+$, and NADPH were each determined using Enzychrom NAD^+/NADH and $NADP^+$/NADPH assay kits (Bioassay Systems, Hayward, CA). Between 0.25 and 1 mL of cultures was removed from the bioreactors at various time points and the biochemical assay was performed as described in the manufacturer's instructions. Concentrations of cofactors were normalized to cell dry weight.

2.8 Proteomic profiling of methyl ketone production strains during fermentation

Proteomic analysis of methyl ketone production strains during fermentation was performed by extracting total proteins and analyzing trypsin-digested peptides, as described elsewhere (González Fernández-Niño et al., 2015). LC-MS/MS shotgun proteomic analyses of the trypsin-digested samples and subsequent protein identification were performed by the UC Davis Genome Center, Proteome Core group (Davis, CA) as previously described (Zargar et al., 2016).

The resulting protein matches were further filtered and validated using Scaffold (version Scaffold_4.7.3, Proteome Software Inc., Portland, OR). Protein identifications were accepted if they could be established at >95.0% probability and contained at least 1 identified peptide (at

99% and greater). This resulted in false discovery rates (FDR) of 3.9% for protein and 0.1% for peptides. After filtering the data with Scaffold, identified proteins that had a normalized weighted spectra value >10 in at least one sample were then exported into R for statistical analysis. In some samples, certain proteins of interest (in particular, Rex and Al_FabG in strain EGS1895) exhibited zero spectral counts. These data were assigned an arbitrary value of 0.5 rather than 0 to preclude calculation of a ratio with a 0 denominator.

3. Results and Discussion

3.1 Optimization of fed-batch fermentation for methyl ketone production in strain EGS1895

Previously, we demonstrated up to 3.4 g/L of methyl ketone production at 45 hr by fed-batch fermentation of strain EGS1895 (with a yield of 0.042 g MK/g glucose), but methyl ketone production stalled after 45 hr despite continued feeding of glucose (Goh et al., 2014). In this study, we attempted to improve and prolong methyl ketone production by modifying the fed-batch fermentation process. Key adjustments to the fermentation process included the following: (1) constant glucose feeding rather than pulsed feeding that was feedback-regulated by DO levels, (2) maintaining higher DO in the bioreactors, and (3) lowering concentration of NH_4Cl in the batch medium from 0.2 g/g of glucose to 0.05 g/g of glucose and maintaining this ratio throughout fed-batch fermentation. With these modifications, we reached a methyl ketone titer of 4.4 g/L at 55 hr (Figure S2), and more importantly, achieved a yield of 0.14 g MK/g glucose (ca. 42% of maximum theoretical yield), which is an improvement over the previously reported fed-batch yield and is comparable to the yield observed in shake-flask experiments. However, as in previous fermentations, methyl ketone production started to plateau after 55 hr (Figure S2). In fact, when methyl ketone production plateaued, glucose consumption and cell growth continued unabated, suggesting a physiological change in strain EGS1895 that led to the cessation of

methyl ketone production. The suspicion that cofactor imbalance, and specifically NADPH limitation and net NADH accumulation, might have triggered this apparent physiological change led us to investigate whether use of an NADH-dependent version of FabG would enable sustained methyl ketone production.

3.2 Overexpressing A. laidlawii FabG improves methyl ketone production in shake-flask experiments

Since the bulk of NADPH consumed during fatty acid biosynthesis is accounted for by FabG-catalyzed reduction of β-ketoacyl-ACPs to β-hydroxyacyl-ACPs, one potential strategy for improving methyl ketone production is to change the cofactor requirement of FabG from NADPH to NADH. In 2014, four different FabG variants (from *Acholeplasma laidlawii* PG-8A, *Bacillus* sp. SG-1, *Cupriavidus taiwanensis* LMG 19424, and *Plesiocystis pacifica* SIR-1) were identified as candidates having greater preference for NADH than NADPH, and this was experimentally verified *in vitro* (Javidpour et al., 2014). We set out to examine whether overexpression of any of these FabG variants would improve methyl ketone production under aerobic conditions. Thus, the FabG variants (and an RFP control) were each expressed in a medium-copy p15a origin of replication (*ori*) plasmid, which was co-transformed with the high-copy ColE1 *ori* plasmid (pEG1675; Goh et al. 2014) that contained the methyl ketone pathway genes (Table I). In addition, we placed the *fabG* variants under the transcriptional control of the *adhE* promoter and its corresponding transcriptional repressor, Rex, from *Staphylococcus aureus* RN4220 (Pagels et al., 2010). Regulation by the Rex repressor is modulated by the $NADH/NAD^+$ ratio: transcription is repressed under a low intracellular ratio and activated under a high intracellular ratio (McLaughlin et al., 2010; Pagels et al., 2010). Thus, placing the FabG variants under the regulation of Rex allowed us to modulate the expression of NADH-dependent

FabG based upon the intracellular NADH/NAD^+ ratio. The red color observed for the RFP control strain (EGS2710) demonstrated that gene expression modulated by the Rex system was occurring under the cultivation conditions.

Among the four different FabG variants overexpressed, only the *A. laidlawii* FabG (Al_FabG), expressed in strain EGS2715 (Table I), showed improvement of methyl ketone production under batch conditions in shake flasks (Figure 1, Table S3). On average, strain EGS2715 had 35% and 75% higher methyl ketone yield than an RFP negative-control strain (EGS2710) in the presence of 1% and 2% glucose, respectively. However, in comparison to strain EGS1895, our best methyl ketone production strain that harbors only a single plasmid (Goh et al. 2014), the improvements were somewhat lower (19% and 40% with 1% and 2% glucose, respectively). It is possible that the lower methyl ketone production in the two-plasmid control strain (EGS2710) relative to the 1-plasmid strain (EGS1895) was the result of a metabolic burden imposed by the second plasmid.

3.3 The two-plasmid methyl ketone production strain is unstable and shows plasmid loss during fed-batch fermentation

Although strain EGS2715 exhibited between 19 to 75% better methyl ketone production than its corresponding control strain, EGS2710, and previous best methyl ketone-producing strain, EGS1895, in shake flasks, we did not observe the same levels of improvement during fed-batch fermentation (Table S4, Figure 2). The average methyl ketone titers for strains EGS2710 and EGS1895 were ca. 4.0 g/L and 3.9 g/L, respectively, while an average methyl ketone titer of ca. 4.4 g/L was achieved for strain EGS2715; this represented only a 10% improvement relative to strain EGS1895.

Plasmid DNA samples were isolated from strain EGS2715 at various time points and analyzed on a DNA agarose gel after restriction enzyme digestion. The agarose gel revealed that some of the expected DNA fragments were not present at later time points, suggesting plasmid loss in the strain over time (Figure 3A). Since the single-plasmid strain, EGS1895, did not show the same plasmid instability (Figure S3), it is evident that the presence of the second plasmid contributed to plasmid instability within the strain. A closer examination of the DNA fragments on the agarose gel reveals that the majority of the DNA fragments lost corresponded to pEG1675, a ColE1-derived plasmid (Table I). Since pEG1675 contains the methyl ketone pathway genes, loss of this plasmid would result in lower expression of the pathway enzymes and consequently, lower methyl ketone production. As expected, we observed that the plateau in methyl ketone production corresponded to times after which plasmid loss was observed (Figure 3B). The loss of ColE1-derived plasmids in the presence of p15a-derived plasmids is not unprecedented. Yao and colleagues showed that co-transformation of ColE1- and p15a-dervived plasmids resulted in the loss of ColE1-derived plasmids and hypothesized that the presence of a p15a-derived plasmid somehow interfered with the proper localization of a ColE1-derived plasmid toward the middle of the cell during replication (Yao et al., 2007).

3.4 Consolidating the A. laidlawii fabG gene and the methyl ketone pathway genes into one plasmid improved plasmid stability and methyl ketone production

Since it was established that the presence of the p15a plasmid led to plasmid instability during fed-batch fermentation, we proceeded to consolidate the *Al_fabG* and the methyl ketone pathway genes into a single plasmid. To accomplish this, the *rex*-P_{adhE}-*Al_fabG* fragment from pEG2695 (Table I) was assembled downstream of the ColE1 *ori* in pEG1675 at the SpeI site (Figure 4A), resulting in plasmid pEG2826 (Figure 4B; Table I). The methyl ketone production

strain EGS2850 harboring plasmid pEG2826 was tested under fed-batch conditions and was found to produce an average of ca. 2.6 g/L of methyl ketones, a titer that was substantially lower than that of strain EGS1895 (Figure 2; Table S4). We then proceeded to alter the location of the *rex*-P_{adhE}-*Al_fabG* fragment, this time cloning the fragment upstream of the ColE1 *ori* at the PciI site, to generate pEG2895 (Figure 4C). The resulting production strain EGS2920, containing plasmid pEG2895, was subsequently tested under fed-batch conditions and attained an average titer of ca. 5.4 g/L over three fermentation runs (Figure 2; Table S4). This represented greater than 2-fold improvement in methyl ketone production over strain EGS2850 and almost 40% improvement over the previous best strain, EGS1895 (Figure 2). Notably, in one of the fermentation runs with strain EGS2920, a methyl ketone titer of ca. 6.0 g/L was achieved (Figure S4), which is the best titer reported for methyl ketones to date.

Proteomic analysis of strains EGS2850 and EGS2920 during fed-batch fermentation revealed that the expression of most methyl ketone pathway enzymes, including FadR, FadD, acyl-CoA oxidase (ACO, or Mlut_11700), and FadB, were, on average, 3.6-fold lower in strain EGS2850 than in strain EGS2920 (Table S5), which readily explains the lower methyl ketone production in strain EGS2850. It is still uncertain why altering the location of the *rex*-P_{adhE}-*Al_fabG* fragment relative to the ColE1 *ori* impacted expression of the other genes on the plasmid, but it has been well documented that, because DNA replication and transcription occur simultaneously, collision between DNA replication machinery and RNA polymerase can disrupt transcription and DNA replication, specifically when these enzymes are oriented head-on (Lin and Pasero, 2012; Mirkin and Mirkin, 2005; Srivatsan et al., 2010). Although this may explain the attenuated expression observed in strain EGS2850, more recently, Bryant and colleagues (2014) observed another potentially relevant phenomenon: when transcription of a reporter

cassette was directed towards another transcription unit downstream, the expression of its neighboring genes was profoundly repressed, irrespective of orientation, due to the supercoiling created ahead of RNA polymerase, which in turn decreased the ability of RNA polymerase to access downstream genes for transcription (Bryant et al., 2014). It is conceivable that the position of the *rex*-P_{adhE}-*Al_fabG* fragment in the first single-plasmid construct (pEG2826; Figure 4B) may have had a similar effect on the transcription of its neighboring genes, while location of the *rex*-P_{adhE}-*Al_fabG* fragment on the second plasmid construct (pEG2895; Figure 4C) precluded this phenomenon.

3.5 Methyl ketone production in fed batch mode in strains with and without NADH-dependent FabG (strains EGS2920 and EGS1895, respectively).

Methyl ketone titer after 145 hr of fed-batch fermentation was ~20% greater for strain EGS2920 than strain EGS1895 (Figure 5A,B), and comparison of the performance of the two strains reveals several interesting trends. First, methyl ketone productivity was initially higher for strain EGS1895 than for strain EGS2920 (e.g., for the first 55 hr), but production plateaued soon thereafter (at ca. 70 hr; Figure 5A). Despite having initially lower productivity, strain EGS2920 sustained methyl ketone production much longer than strain EGS1895 (through 150 hr; Figure 5A) and this accounts for the higher final titer for strain EGS2920. Second, strain EGS1895 accumulated greater amounts of pyruvate and acetate than EGS2920 during fed-batch fermentation. Specifically, EGS1895 showed a steady increase in acetate accumulation throughout fermentation, reaching a final concentration of ca. 6.0 g/L, and had an abrupt increase in pyruvate that co-occurred with the plateauing of methyl ketone production. In contrast, strain EGS2920 had little or no pyruvate accumulation during the entire course of fermentation, while acetate accumulation was consistently below 1 g/L, with a brief spike in acetate near the end of

fermentation that never exceeded 2 g/L, and the acetate was completely re-assimilated after all the glucose was exhausted (Figure 5A). Interestingly, the brief increase in acetate accumulation in strain EGS2920 also corresponded to when methyl ketone production began to plateau.

It is surprising to observe acetate accumulation in strains EGS1895 and EGS2920 even though the major acetate-producing pathways (*ackA-pta* and *poxB*) have been deleted in both strains (Table I). However, Phue and colleagues observed the same phenomenon in *E. coli* BL21 and proposed that other deacetylating enzymes, such as acetoacetyl-CoA transferases (AtoA, AtoD), or cysteine synthases (CysM, CysK), could contribute to the accumulation of acetate in such strains (Phue et al., 2010). In fact, according to EcoCyc (http://ecocyc.org), there are at least 10 alternate enzymes in *E. coli* that catalyze acetate-producing reactions. Based upon our shotgun proteomics data, AldB, which converts acetaldehyde to acetate while generating a molecule of NADPH, and NagA, a *N*-acetylglucosamine-6-phosphate deacetylase, were both detected and are potential sources of acetate (Supplementary Data File S1).

3.6 Proteomic profiles of strains EGS2920 and EGS1895 during fed-batch fermentation

To better understand the physiological differences that led to improved methyl ketone production in strain EGS2920 relative to strain EGS1895, we analyzed the proteomic profiles of both strains. Proteins that were at least 1.5-fold significantly ($p \leq 0.05$) upregulated or downregulated in strain EGS2920 compared to EGS1895 are summarized in Supplementary Data File S1 and volcano plots highlighting the differential expression of proteins at various time points (50 hr, 70 hr, and 120 hr) are displayed in Figure 6. As expected, the two most highly upregulated proteins in strain EGS2920 at all times were Rex and Al_FabG, since these proteins are not present in strain EGS1895.

Since our engineering strategy for using NADH-dependent FabG (Al_FabG) was predicated on alleviating NADPH limitation, we examined the proteomic data for evidence of whether NADPH demand was indeed alleviated in strain EGS2920. Table II lists key *E. coli* enzymes involved in NADPH production (Csonka and Fraenkel, 1977) and their differential expression in strains EGS1895 and EGS2920. Most of these proteins do not show significant differential expression, but Pgi (glucose-6-phosphate isomerase) was significantly (typically $p \leq 0.05$ across all time points) upregulated in strain EGS2920, whereas MaeB (a $NADP^+$-dependent malate dehydrogenase) was significantly downregulated in EGS2920 (at 50 and 70 hr). Although Pgi is not a NADPH-generating enzyme *per se*, it drives flux towards glycolysis and away from the NADPH-generating oxidative branch of the pentose phosphate pathway (PPP). This increase in Pgi expression, along with lower expression of MaeB, in strain EGS2920 suggests that there might be a lower demand for NADPH in this strain than in strain EGS1895. These results are consistent with those of bioassays for intracellular NADPH and $NADP^+$, which showed higher $NADPH/NADP^+$ ratios for strain EGS2920 than EGS1895 (Figure S5A) but no consistent trend for $NADH/NAD^+$ ratio (Figure S5B) throughout most of the fed-batch fermentation. Increased flux through glycolysis is also suggested by the upregulation of a subset of Cra-repressed proteins in strain EGS2920 (Table S6). Fructose 1,6-bisphosphate (FBP), a known effector of the Cra regulator (Chin et al., 1989; Ramseier et al., 1995; Shimada et al., 2005), is also a downstream product of the Pgi-catalyzed reaction. Increased expression of Pgi likely increased intracellular concentration of FBP, which would allow for FBP to interact with Cra and induce a conformational change that released Cra from the transcriptional repression of these Cra-regulated proteins.

In addition to the NADPH demand from fatty acid biosynthesis, oxidative stress response, as indicated by the high expression of catalases (KatE, KatG) and the alkyl hydroperoxide reductase (AhpCF) in both strains (Supplementary Data File S1), may also have added to the cellular demand for NADPH. Stimulation of the oxidative stress response in these engineered strains is not surprising since the overexpressed acyl-CoA oxidase (ACO) enzyme (encoded by Mlut_11700) generates H_2O_2 as part of the reaction it catalyzes, namely, oxidation of an acyl-CoA to an enoyl-CoA (Figure S1). It has been well documented that (1) NADPH is important for defense against oxidative stress, as it plays an important role in regenerating the oxidized glutathione, thioredoxin, and glutaredoxin systems involved in maintaining disulfide bridges in proteins and in protection from oxygen radicals (Carmel-Harel and Storz, 2000; Izawa et al., 1995; Prinz et al., 1997) and (2) mutations that disrupt the PPP result in cells being more susceptible to oxidative stress, presumably due to lack of NADPH regeneration (Juhnke et al., 1996; Rungrassamee et al., 2008; Sandoval et al., 2011). Therefore, overexpression of the Al_FabG in strain EGS2920 may not just be relieving the NADPH demand for methyl ketone synthesis but also making more NADPH available for combatting H_2O_2-mediated oxidative stress, all of which may contribute to improved methyl ketone production.

Another group of stress-related proteins showed strong differential expression in this study, and were expressed much more highly in strain EGS1895 than in strain EGS2920: these include glutamate decarboxylase (GadA, GadB, GadC) and the maltose transporter (MalE) (Table S6), which have been related to acid stress (Maurer et al., 2005). Although the differential expression may simply be a direct result of increased organic acid (e.g., acetate, pyruvate, lactate) production in strain EGS1895, these genes are also known to have overlapping response to oxidative stress (Basak and Jiang, 2012; Maurer et al., 2005; Zheng et al., 2001). Thus, it is

also possible that the shortage of NADPH in strain EGS1895 elicited a stronger oxidative stress response.

Proteomic analysis may also provide further information about why methyl ketone production plateaued in both strain EGS1895 and EGS2920 (albeit at different times) despite continued glucose consumption and growth during the plateau period (Figure 5). As just discussed, there are indications that limited NADPH availability compromised strain EGS1895 relative to strain EGS2920 throughout much of the fermentation period. However, there may have been some common physiological and stress-related phenomena that were shared by both strains during their plateau phases (after ~70 hr for EGS1895 and after ~120 hr for EGS2920; Figure 5A). We examined proteomic profiles during these periods by normalizing all protein abundances for each strain at 70 and 120 hr relative to those at 50 hr (Supplementary Data File S2) and focused on upregulation or downregulation patterns common to the plateaus in both strains (strain EGS1895 at 70 and 120 hr and strain EGS2920 at 120 hr) but not common to strain EGS2920 at 70 hr, at which time methyl ketone production was still occurring (Figure 5A). We found that, for both strains, certain stress-related proteins were more upregulated during the plateau period than during the productive period (typically $p < 0.01$), including GadA and GadB (glutamate decarboxylase subunits, already discussed), HdeA and HdeB (acid-stress chaperones), and the universal stress protein, UspA (Figure S6A). So, while strain EGS1895 may have undergone more stress due to NADPH limitations throughout fermentation, both strains EGS1895 and EGS2920 were undergoing some similar stresses during the plateau period. In addition, an important protein involved in fatty acid biosynthesis (AccB, or acetyl-CoA carboxylase subunit B) was markedly (5- to 6-fold) downregulated in both strains (Figure S6B) during their plateau periods ($p < 0.002$). As fatty acids are methyl ketone precursors, disruption

of fatty acid synthesis after ~70 hr (strain EGS1895) or ~120 hr (EGS2920) could have affected methyl ketone production.

Shotgun proteomics profiling provided us with global insights into the physiological state of methyl ketone production strains, and will serve to guide strain optimization efforts in the future. In particular, proteomics data indicated that oxidative stress (perhaps in part from pathway-derived H_2O_2) may play an important role during methyl ketone production and therefore, enhancing tolerance to oxidative stress may be critical to prolonging and enhancing methyl ketone production during fed-batch fermentation.

Acknowledgments

We thank Michelle Salemi (Proteome Core group, U.C. Davis Genome Center) for mass spectrometric analysis of protein samples. This work conducted by the Joint BioEnergy Institute was supported by the Office of Science, Office of Biological and Environmental Research, of the U.S. Department of Energy under Contract No. DE-AC02-05CH11231. J.D.K. has a financial interest in Amyris and Lygos, Demetrix, and Constructive Biology.

References

Auriol, C., Bestel-Corre, G., Claude, J.-B., Soucaille, P., Meynial-Salles, I., 2011. Stress-induced evolution of *Escherichia coli* points to original concepts in respiratory cofactor selectivity. *Proc. Natl. Acad. Sci. U. S. A.* 108, 1278–83. doi:10.1073/pnas.1010431108

Basak, S., Jiang, R., 2012. Enhancing *E. coli* tolerance towards oxidative stress via engineering its global regulator cAMP receptor protein (CRP). *PLoS One* 7, e51179. doi:10.1371/journal.pone.0051179

Beller, H.R., Lee, T.S., Katz, L., 2015. Natural products as biofuels and bio-based chemicals: fatty acids and isoprenoids. *Nat. Prod. Rep.* 32, 1508–1526. doi:10.1039/C5NP00068H

Bergler, H., Fuchsbichler, S., Hogenauer, G., Turnowsky, F., 1996. The enoyl-[acyl-carrier-protein] reductase (FabI) of *Escherichia coli*, which catalyzes a key regulatory step in fatty acid biosynthesis, accepts NADH and NADPH as cofactors and is inhibited by palmitoyl-CoA. *Eur. J. Biochem.* 242, 689–694. doi:10.1111/j.1432-1033.1996.0689r.x

Bryant, J.A., Sellars, L.E., Busby, S.J.W., Lee, D.J., 2014. Chromosome position effects on gene expression in *Escherichia coli* K-12. *Nucleic Acids Res.* 42, 11383–92. doi:10.1093/nar/gku828

Carmel-Harel, O., Storz, G., 2000. Roles of the glutathione- and thioredoxin-dependent reduction systems in the *Escherichia coli* and *Saccharomyces cerevisiae* responses to oxidative stress. *Annu. Rev. Microbiol.* 54, 439–461. doi:10.1146/annurev.micro.54.1.439

Chin, A.M., Feldheim, D.A., Saier, M.H., 1989. Altered transcriptional patterns affecting several metabolic pathways in strains of *Salmonella typhimurium* which overexpress the fructose regulon. *J. Bacteriol.* 171, 2424–34. doi:10.1128/JB.171.5.2424-2434.1989

Chou, H.H., Marx, C.J., Sauer, U., 2015. Transhydrogenase promotes the robustness and

evolvability of *E. coli* deficient in NADPH production. *PLoS Genet.* 11, e1005007. doi:10.1371/journal.pgen.1005007

Csonka, L.N., Fraenkel, D.G., 1977. Pathways of NADPH formation in *Escherichia coli*. *J. Biol. Chem.* 252, 3382–91.

Gibson, D.G., Young, L., Chuang, R.-Y., Venter, J.C., Hutchison, C.A., Smith, H.O., 2009. Enzymatic assembly of DNA molecules up to several hundred kilobases. *Nat. Methods* 6, 343–5. doi:10.1038/nmeth.1318

Goh, E.-B., Baidoo, E.E.K., Burd, H., Lee, T.S., Keasling, J.D., Beller, H.R., 2014. Substantial improvements in methyl ketone production in *E. coli* and insights on the pathway from in vitro studies. *Metab. Eng.* 26C, 67–76. doi:10.1016/j.ymben.2014.09.003

Goh, E.-B., Baidoo, E.E.K., Keasling, J.D., Beller, H.R., 2012. Engineering of bacterial methyl ketone synthesis for biofuels. *Appl. Environ. Microbiol.* 78, 70–80. doi:10.1128/AEM.06785-11

González Fernández-Niño, S.M., Smith-Moritz, A.M., Chan, L.J.G., Adams, P.D., Heazlewood, J.L., Petzold, C.J., 2015. Standard flow liquid chromatography for shotgun proteomics in bioenergy research. *Front. Bioeng. Biotechnol.* 3, 44. doi:10.3389/fbioe.2015.00044

Handke, P., Lynch, S.A., Gill, R.T., 2011. Application and engineering of fatty acid biosynthesis in *Escherichia coli* for advanced fuels and chemicals. *Metab. Eng.* 13, 28–37. doi:10.1016/j.ymben.2010.10.007

Izawa, S., Inoue, Y., Kimura, A., 1995. Oxidative stress response in yeast: effect of glutathione on adaptation to hydrogen peroxide stress in *Saccharomyces cerevisiae*. *FEBS Lett.* 368, 73–76. doi:10.1016/0014-5793(95)00603-7

Janßen, H., Steinbüchel, A., 2014. Fatty acid synthesis in *Escherichia coli* and its applications

towards the production of fatty acid based biofuels. *Biotechnol. Biofuels* 7, 7. doi:10.1186/1754-6834-7-7

Javidpour, P., Pereira, J.H., Goh, E.-B., McAndrew, R.P., Ma, S.M., Friedland, G.D., Keasling, J.D., Chhabra, S.R., Adams, P.D., Beller, H.R., 2014. Biochemical and structural studies of NADH-dependent FabG used to increase the bacterial production of fatty acids under anaerobic conditions. *Appl. Environ. Microbiol.* 80, 497–505. doi:10.1128/AEM.03194-13

Juhnke, H., Krems, B., Kotter, P., Entian, K.-D., 1996. Mutants that show increased sensitivity to hydrogen peroxide reveal an important role for the pentose phosphate pathway in protection of yeast against oxidative stress. *MGG Mol. Gen. Genet.* 252, 456–464. doi:10.1007/BF02173011

Korz, D.J., Rinas, U., Hellmuth, K., Sanders, E.A., Deckwer, W.-D., 1995. Simple fed-batch technique for high cell density cultivation of *Escherichia coli*. *J. Biotechnol.* 39, 59–65. doi:10.1016/0168-1656(94)00143-Z

Kreiswirth, B.N., Löfdahl, S., Betley, M.J., O'Reilly, M., Schlievert, P.M., Bergdoll, M.S., Novick, R.P., 1983. The toxic shock syndrome exotoxin structural gene is not detectably transmitted by a prophage. *Nature* 305, 709–712. doi:10.1038/305709a0

Lee, H.C., Kim, J.S., Jang, W., Kim, S.Y., 2009. Thymidine production by overexpressing NAD^+ kinase in an *Escherichia coli* recombinant strain. *Biotechnol. Lett.* 31, 1929–1936. doi:10.1007/s10529-009-0097-z

Lee, T.S., Krupa, R.A., Zhang, F., Hajimorad, M., Holtz, W.J., Prasad, N., Lee, S.K., Keasling, J.D., 2011. BglBrick vectors and datasheets: A synthetic biology platform for gene expression. *J. Biol. Eng.* 5, 12. doi:10.1186/1754-1611-5-12

Lee, W.-H., Kim, M.-D., Jin, Y.-S., Seo, J.-H., 2013. Engineering of NADPH regenerators in

Escherichia coli for enhanced biotransformation. *Appl. Microbiol. Biotechnol.* 97, 2761–2772. doi:10.1007/s00253-013-4750-z

Lennen, R.M., Pfleger, B.F., 2013. Microbial production of fatty acid-derived fuels and chemicals. *Curr. Opin. Biotechnol.* 24, 1044–1053. doi:10.1016/j.copbio.2013.02.028

Lin, Y.-L., Pasero, P., 2012. Interference between DNA replication and transcription as a cause of genomic instability. *Curr. Genomics* 13, 65–73. doi:10.2174/138920212799034767

Maurer, L.M., Yohannes, E., Bondurant, S.S., Radmacher, M., Slonczewski, J.L., 2005. pH regulates genes for flagellar motility, catabolism, and oxidative stress in *Escherichia coli* K-12. *J. Bacteriol.* 187, 304–19. doi:10.1128/JB.187.1.304-319.2005

McLaughlin, K.J., Strain-Damerell, C.M., Xie, K., Brekasis, D., Soares, A.S., Paget, M.S.B., Kielkopf, C.L., 2010. Structural basis for NADH/NAD^+ redox sensing by a Rex family repressor. *Mol. Cell* 38, 563–575. doi:10.1016/j.molcel.2010.05.006

Meselson, M., Yuan, R., 1968. DNA restriction enzyme from *E. coli*. *Nature* 217, 1110–1114. doi:10.1038/2171110a0

Mirkin, E. V, Mirkin, S.M., 2005. Mechanisms of transcription-replication collisions in bacteria. *Mol. Cell. Biol.* 25, 888–95. doi:10.1128/MCB.25.3.888-895.2005

Pagels, M., Fuchs, S., Pané-Farré, J., Kohler, C., Menschner, L., Hecker, M., McNamarra, P.J., Bauer, M.C., von Wachenfeldt, C., Liebeke, M., Lalk, M., Sander, G., von Eiff, C., Proctor, R.A., Engelmann, S., 2010. Redox sensing by a Rex-family repressor is involved in the regulation of anaerobic gene expression in *Staphylococcus aureus*. *Mol. Microbiol.* 76, 1142–61. doi:10.1111/j.1365-2958.2010.07105.x

Phue, J.-N., Lee, S.J., Kaufman, J.B., Negrete, A., Shiloach, J., 2010. Acetate accumulation through alternative metabolic pathways in *ackA* − *pta* − *poxB* − triple mutant in *E. coli* B

(BL21). *Biotechnol. Lett.* 32, 1897–1903. doi:10.1007/s10529-010-0369-7

Prinz, W.A., Aslund, F., Holmgren, A., Beckwith, J., 1997. The role of the thioredoxin and glutaredoxin pathways in reducing protein disulfide bonds in the *Escherichia coli* cytoplasm. *J. Biol. Chem.* 272, 15661–7. doi:10.1074/JBC.272.25.15661

Ramseier, T.M., Bledig, S., Michotey, V., Feghali, R., Saier, M.H., 1995. The global regulatory protein FruR modulates the direction of carbon flow in *Escherichia coli*. *Mol. Microbiol.* 16, 1157–1169. doi:10.1111/j.1365-2958.1995.tb02339.x

Rungrassamee, W., Liu, X., Pomposiello, P.J., 2008. Activation of glucose transport under oxidative stress in *Escherichia coli*. *Arch. Microbiol.* 190, 41–9. doi:10.1007/s00203-008-0361-y

Sambrook, J., Fritsch, E.F., Maniatis, T., 1989. Molecular cloning: a laboratory manual, 2nd ed. Cold Spring Harbor Laboratory, Cold Spring Harbor, N.Y.

Sandoval, J.M., Arenas, F.A., Vásquez, C.C., Purwantini, E., Daniels, L., 2011. Glucose-6-phosphate dehydrogenase protects *Escherichia coli* from tellurite-mediated oxidative stress. *PLoS One* 6, e25573. doi:10.1371/journal.pone.0025573

Shimada, T., Fujita, N., Maeda, M., Ishihama, A., 2005. Systematic search for the Cra-binding promoters using genomic SELEX system. *Genes to Cells* 10, 907–918. doi:10.1111/j.1365-2443.2005.00888.x

Spaans, S.K., Weusthuis, R.A., van der Oost, J., Kengen, S.W.M., 2015. NADPH-generating systems in bacteria and archaea. *Front. Microbiol.* 6, 742. doi:10.3389/fmicb.2015.00742

Srivatsan, A., Tehranchi, A., MacAlpine, D.M., Wang, J.D., Olmedo, G., 2010. Co-orientation of replication and transcription preserves genome integrity. *PLoS Genet.* 6, e1000810. doi:10.1371/journal.pgen.1000810

Steen, E.J., Kang, Y., Bokinsky, G., Hu, Z., Schirmer, A., McClure, A., del Cardayre, S.B., Keasling, J.D., 2010. Microbial production of fatty-acid-derived fuels and chemicals from plant biomass. *Nature* 463, 559–562. doi:10.1038/nature08721

Toomey, R.E., Wakil, S.J., 1966. Studies on the mechanism of fatty acid synthesis XV. Preparation and general properties of β-ketoacyl acyl carrier protein reductase from *Escherichia coli*. *Biochim. Biophys. Acta* - Lipids Lipid Metab. 116, 189–197. doi:10.1016/0005-2760(66)90001-4

Wang, Y., San, K.-Y., Bennett, G.N., 2013. Cofactor engineering for advancing chemical biotechnology. *Curr. Opin. Biotechnol.* 24, 994–999. doi:10.1016/j.copbio.2013.03.022

Yao, S., Helinski, D.R., Toukdarian, A., 2007. Localization of the naturally occurring plasmid ColE1 at the cell pole. *J. Bacteriol.* 189, 1946–53. doi:10.1128/JB.01451-06

Zargar, K., Saville, R., Phelan, R.M., Tringe, S.G., Petzold, C.J., Keasling, J.D., Beller, H.R., 2016. *In vitro* characterization of phenylacetate decarboxylase, a novel enzyme catalyzing toluene biosynthesis in an anaerobic microbial community. *Sci. Rep.* 6, 31362. doi:10.1038/srep31362

Zerez, C.R., Moul, D.E., Gomez, E.G., Lopez, V.M., Andreoli, A.J., 1987. Negative modulation of *Escherichia coli* NAD kinase by NADPH and NADH. *J. Bacteriol.* 169, 184–8. doi:10.1128/JB.169.1.184-188.1987

Zhang, F., Carothers, J.M., Keasling, J.D., 2012. Design of a dynamic sensor-regulator system for production of chemicals and fuels derived from fatty acids. *Nat. Biotechnol.* 30, 354–9. doi:10.1038/nbt.2149

Zheng, M., Wang, X., Templeton, L.J., Smulski, D.R., Larossa, R.A., Storz, G., 2001. DNA microarray-mediated transcriptional profiling of the *Escherichia coli* response to hydrogen

peroxide. *J. Bacteriol.* 183, 4562. doi:10.1128/JB.183.15.4562

Supporting Information

Appendix A. Supplementary Tables and Figures

Supplementary Data File S1. Shotgun proteomics data supporting Figure 6

Supplementary Data File S2. Shotgun proteomics data supporting Figure S6

Table Captions

Table I. Bacterial strains and plasmids used in this study.

Table II. Differential expression of key enzymes that impact generation of NADPH in *E. coli*.

Table I. Bacterial strains and plasmids used in this study

Strain or plasmid	Relevant Characteristics	Source or reference
E. coli strains		
DH1	*endA1 recA1 gyrA96 thi-1 glnV44 relA1 hsdR*17(r_K^- m_K^+) λ^-	(Meselson and Yuan, 1968)
LT-ΔfadE	DH1 Δ*fadE* with pKS1	(Steen et al., 2010)
EGS1405	LT-Δ*fadE*, Δ*poxB*, Δ*ackA-pta*	
EGS1895	EGS1405 with pEG1675	(Goh et al., 2014)
EGS2710	EGS1405 with pEG1675 and pEG2650	This study
EGS2715	EGS1405 with pEG1675 and pEG2695	This study
EGS2720	EGS1405 with pEG1675 and pEG2700	This study
EGS2725	EGS1405 with pEG1675 and pEG2705	This study
EGS2735	EGS1405 with pEG1675 and pEG2730	This study
EGS2850	EGS1405 with pEG2826	This study
EGS2920	EGS1405 with pEG2895	This study
PJ002	BL21(DE3) with pPJ101	(Javidpour et al., 2014)
PJ003	BL21(DE3) with pPJ102	(Javidpour et al., 2014)
PJ004	BL21(DE3) with pPJ104	(Javidpour et al., 2014)
PJ005	BL21(DE3) with pPJ103	(Javidpour et al., 2014)
Other strains		
S. aureus RN4220	A strain with partial *agr* defect, selected for transformability with DNA from *E. coli*	(Kreiswirth et al., 1983)

Plasmids		
pBbA5c-RFP	Cm^r; p15a derivative containing RFP under the lactose promoter (P_{lacUV5}).	(Lee et al., 2011)
pBbE8k-RFP	Km^r; ColE1 derivative containing RFP under the arabinose promoter (P_{BAD}).	(Lee et al., 2011)
pEG1675	Km^r, ColE1-derived plasmid with the entire methyl ketone pathway expressed.	(Goh et al., 2014)
pEG2650	Cm^r, Gibson assembly of the 636-bp *rex* gene and 85-bp *adhE* promoter (P_{adhE}) region from *S. aureus* into pBbA5c-RFP at the SalI and EcoRI sites.	This study
pEG2695	Cm^r; Gibson assembly of the 723-bp *fabG* gene from pJP101 into pEG2650 at the NdeI and BamHI	This study
pEG2700	Cm^r; Gibson assembly of the 741-bp *fabG* gene from pJP104 into pEG2650 at the NdeI and BamHI	This study
pEG2705	Cm^r; Gibson assembly of the 774-bp *fabG* gene from pJP103 into pEG2650 at the NdeI and BamHI	This study
pEG2730	Cm^r; Gibson assembly of the 732-bp *fabG* gene from pJP102 into pEG2650 at the NdeI and BamHI	This study
pEG2826	Km^r, Gibson assembly of ~1.7-kb fragment of *rex*-P_{adhE}-*Al_fabG* fragment from pEG2695 into EG1675 at the SpeI sites.	This study
pEG2895	Km^r, Gibson assembly of ~1.7-kb fragment of *rex*-P_{adhE}-*Al_fabG* fragment from pEG2695 into pEG1675 at the PciI sites.	This study
pPJ101	Km^r, *fabG* gene from *Acholeplasma laidlawii* PG-8A cloned into pET24(+) vector	(Javidpour et al., 2014)
pPJ102	Km^r, *fabG* gene from *Bacillus* sp. SG-1 cloned into pET24(+) vector	(Javidpour et al., 2014)

pPJ103	Km^r, *fabG* gene from *Plesiocystis pacifica* SIR-1 cloned into pET24(+) vector	(Javidpour et al., 2014)
pPJ104	Km^r, *fabG* gene from *Cupriavidus taiwanensis* LMG 19424 cloned into pET24 vector	(Javidpour et al., 2014)

Table II. Differential expression of key enzymes that impact generation of NADPH in *E. coli*

Enzyme	Pathway	Protein fold change[a]			p-value		
		50h	70h	120h	50h	70h	120h
Pgi	Glycolysis	2.0	1.5	1.8	$4.3x10^{-3}$	$1.8 x10^{-4}$	$1.1 x10^{-5}$
Zwf	PPP	1.5	1.3	1.1	$1.3 x10^{-3}$	$1.3 x10^{-2}$	$4.1 x10^{-1}$
Gnd	PPP	1.0	1.0	0.85	$7.5 x10^{-1}$	$8.9 x10^{-1}$	$5.0 x10^{-2}$
Icd	TCA	1.1	1.1	0.96	$3.8 x10^{-1}$	$6.4 x10^{-1}$	$1.4 x10^{-1}$
MaeB	TCA	0.26	0.51	2.0	$6.3 x10^{-2}$	$5.4 x10^{-2}$	$1.5 x10^{-2}$
PntA	Transhydrogenase	0.79	0.80	1.1	$3.9 x10^{-2}$	$3.8 x10^{-1}$	$6.2 x10^{-1}$
PntB	Transhydrogenase	0.78	0.48	0.61	$5.6 x10^{-2}$	$1.7 x10^{-1}$	$3.0 x10^{-1}$

[a]Protein fold change is based on the ratio of normalized weighted spectra for the protein in strain EGS2920 relative to that in the reference strain (EGS1895) at three time points.

FIGURE LEGENDS

Figure 1 Methyl ketone yields of strains overexpressing the alternate FabGs from *A. laidlawii* (EGS2715), *C. taiwanensis* (EGS2720), *P. pacifica* (EGS2725), *Bacillus* sp. SG-1 (EGS2735), and an RFP control (represented in red; EGS2710) at 96 hr. Methyl ketone yield is normalized to EGS1895 (represented in black) with 1% glucose (lighter shade) and 2% glucose (darker shade), respectively. Error bars represent 1 standard deviation.

Figure 2 Average methyl ketone titer after 200 hr of fed-batch fermentation for selected methyl ketone-producing strains. Gray bars represent strains containing two plasmids and black bars represent strains containing one plasmid. Error bars represent 1 standard deviation.

Figure 3 (A) DNA electrophoresis gel of plasmid samples (200 ng) extracted from strain EGS2715 at various time points (indicated in hr) during fed-batch fermentation and digested with BamHI and EcoRI. Red arrows indicate DNA bands corresponding to pEG1675 that are missing after 120 hr of fermentation. (B) Methyl ketone titer of strain EGS2715 during fermentation; the blue arrow indicates detection of plasmid loss, which corresponded to a plateau in methyl ketone titer.

Figure 4 Vector maps of (A) pEG1675 plasmid and insertion of the *rex*-P_{adhE}-*Al_fabG* fragment relative to the ColE1 *ori* (highlighted in yellow), resulting in plasmids (B) pEG2826 and (C) pEG2895.

Figure 5 A representative plot of fed-batch fermentation for strains EGS1895 (dashed lines) and EGS2920 (solid lines), showing trends for (A) methyl ketone titers, organic acid production, and cell dry weight (CDW) and (B) consumed glucose and methyl ketone yield.

Figure 6 Volcano plots (p-value vs. $\log_2$ fold differential expression) for proteins detected in strains EGS2920 and EGS1895 at 50, 70, and 120 hr during fed-batch fermentation. Relative fold change for a given protein was calculated as the $\log_2$ ratio of the normalized weighted spectra in strain EGS2920 divided by that in strain EGS1895. Proteins more highly expressed in strain EGS1895 are skewed toward the negative *x* axis, whereas proteins more highly expressed in strain EGS2920 are skewed toward the positive *x* axis. Proteins that have less than 1.5 fold change or are not significantly differentially expressed ($p > 0.05$; below the grey dashed line) are highlighted in grey. Proteins that are significantly ($p \leq 0.05$; above the grey dashed line) and more than 1.5 fold upregulated, or downregulated, in strain EGS2920 are highlighted in green and red, respectively. In addition, key enzymes involved in NADPH generation are highlighted in dark blue, acid/H_2O_2 stress-related proteins are highlighted in light blue, and Cra-regulated proteins are highlighted in purple (see text).

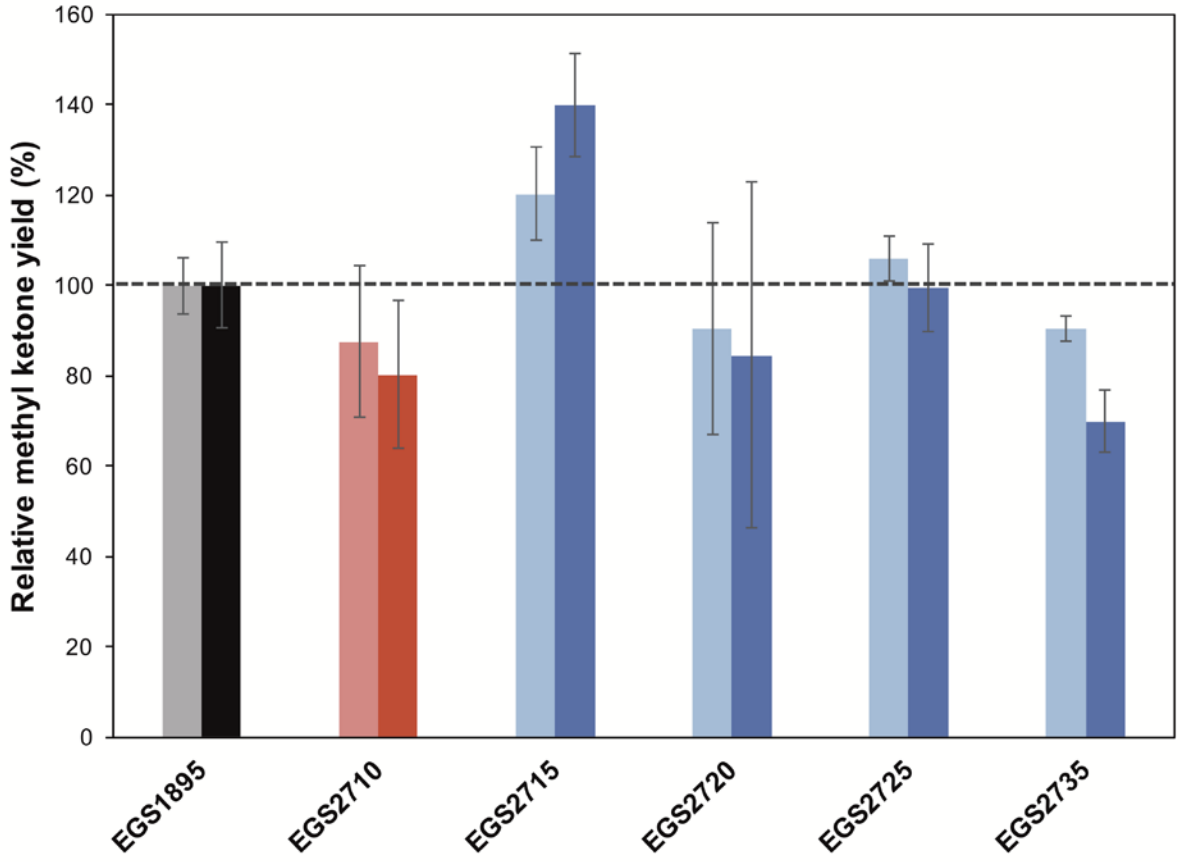

Figure 1

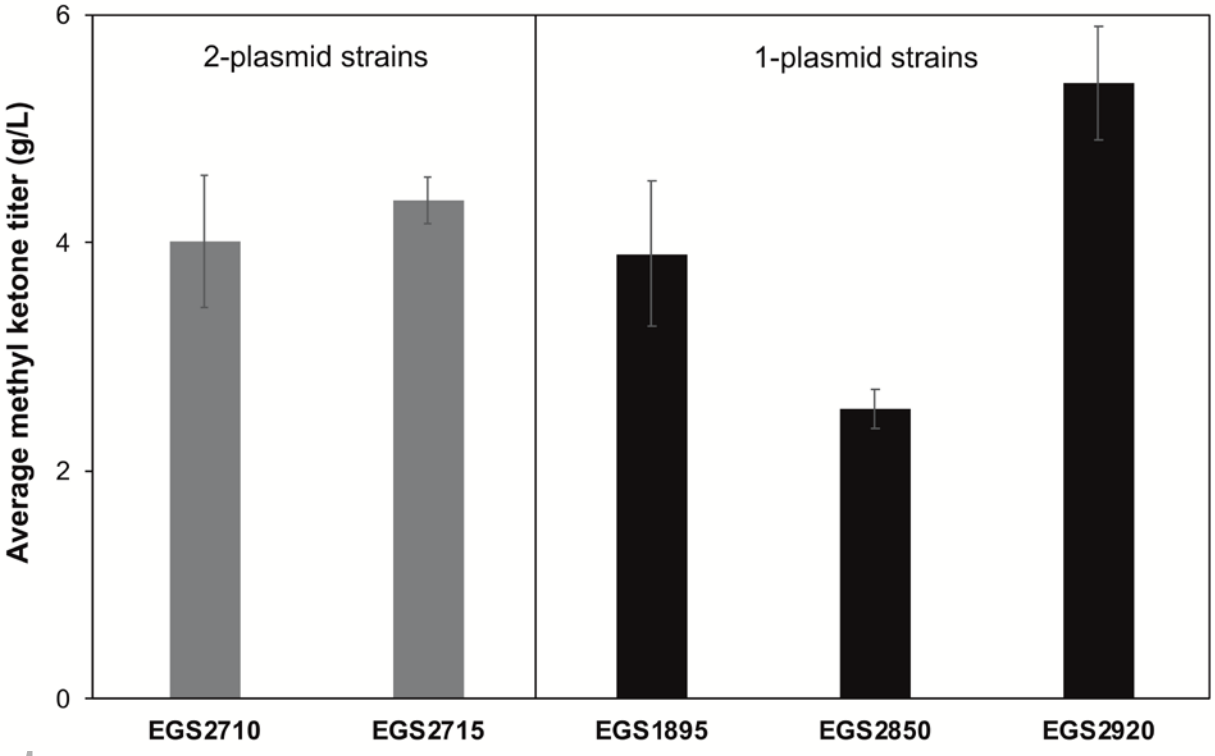

Figure 2

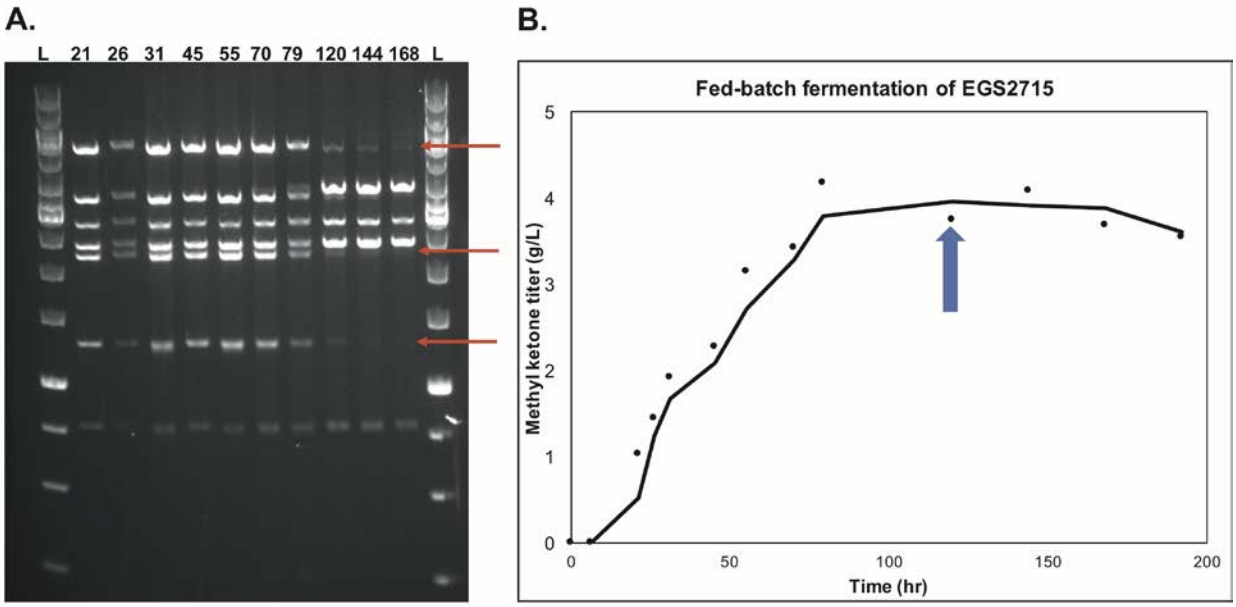

Figure 3

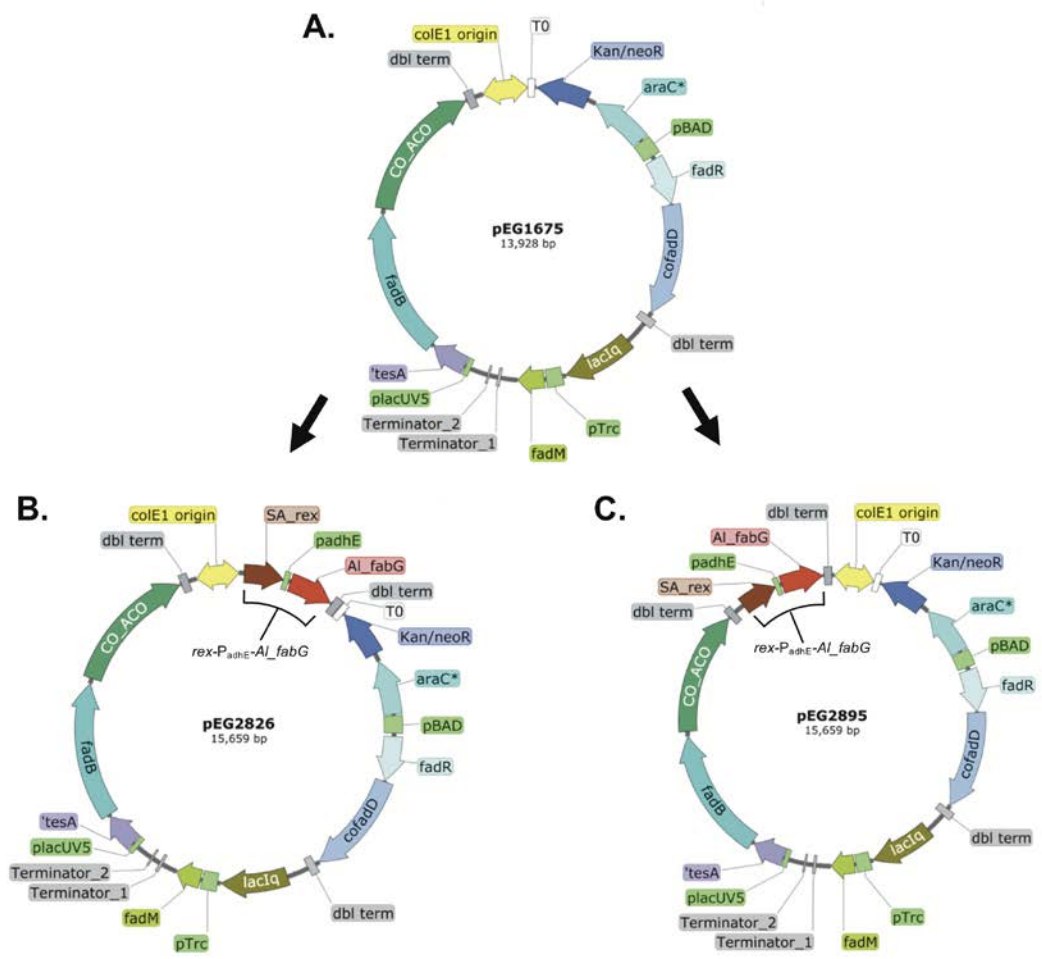

Figure 4

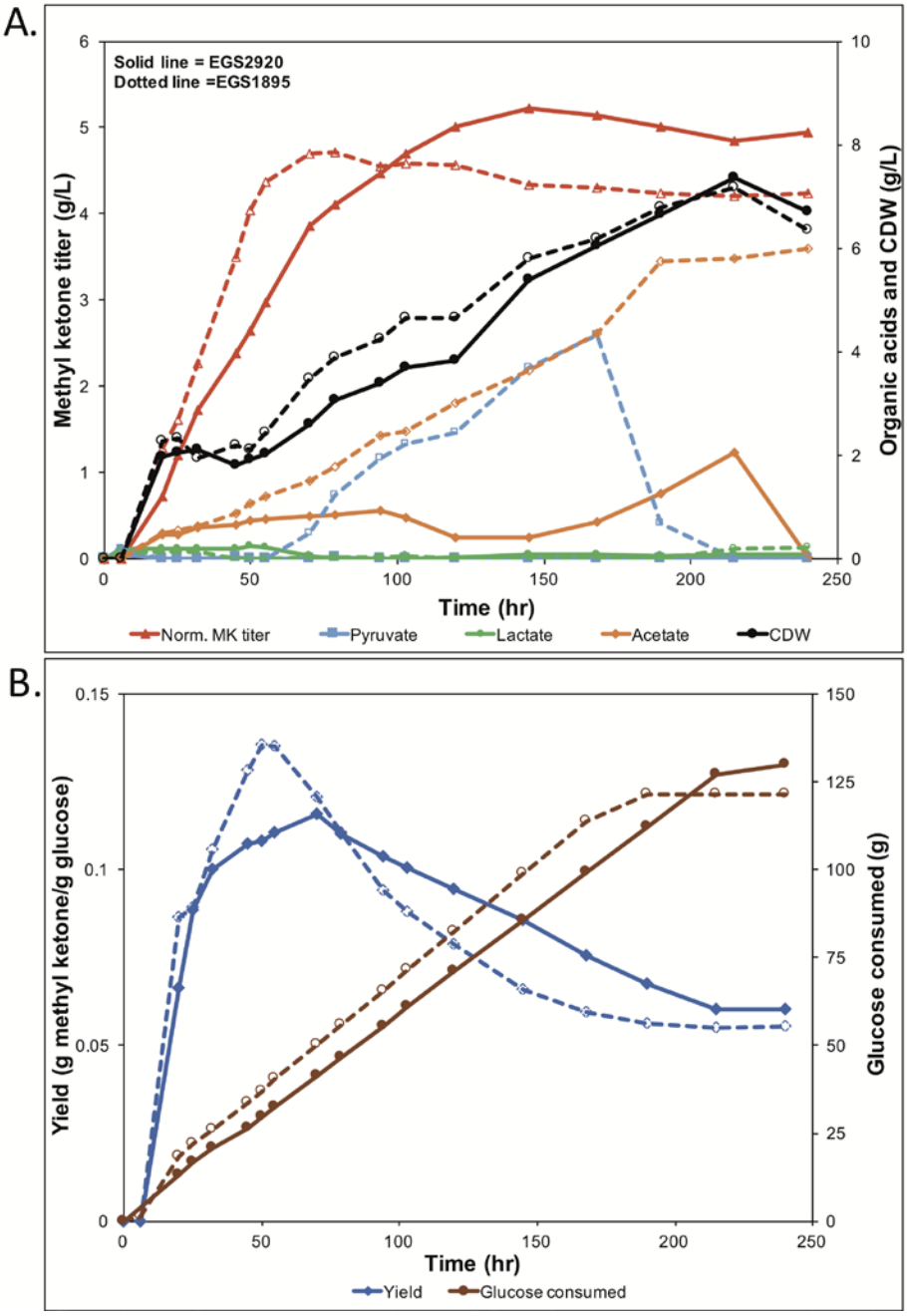

Figure 5

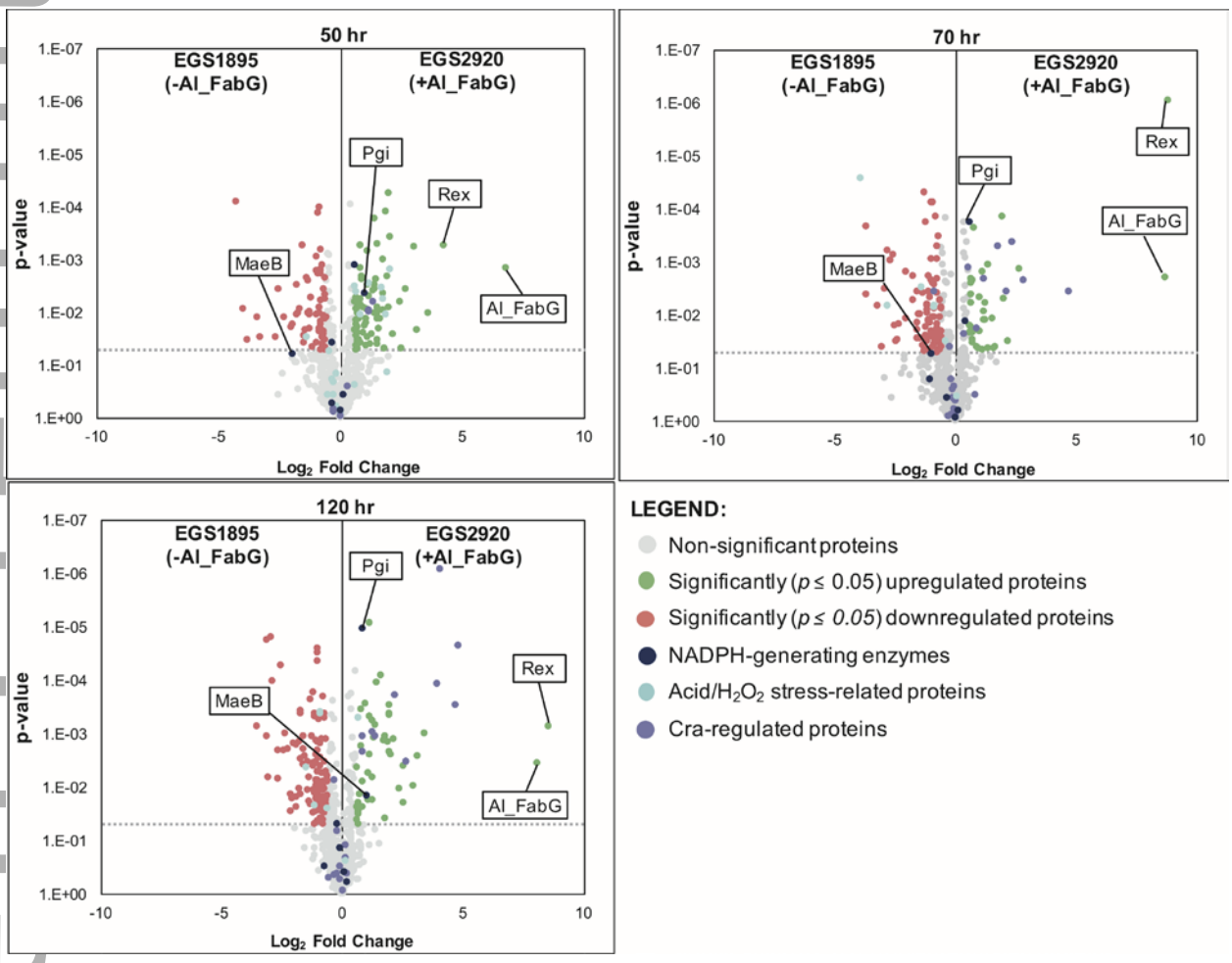

Figure 6